PAPER

Wavelet-based AR–SVM for health monitoring of smart structures

Smart Mater. Struct. **22** (2013) 015003 (12pp) doi:10.1088/0964-1726/22/1/015003

Wavelet-based AR–SVM for health monitoring of smart structures

Yeesock Kim[1], Jo Woon Chong[2], Ki H Chon[3] and JungMi Kim[1]

[1] Civil and Environmental Engineering, Worcester Polytechnic Institute (WPI), Worcester, MA 01609, USA
[2] Laboratory for Information and Decision Systems, Massachusetts Institute of Technology (MIT), Cambridge, MA 02139, USA
[3] Biomedical Engineering, WPI, Worcester, MA 01609, USA

E-mail: yeesock@wpi.edu, jwchong@mit.edu, kichon@wpi.edu and lizkim@wpi.edu

Received 20 June 2012, in final form 5 October 2012
Published 30 November 2012
Online at stacks.iop.org/SMS/22/015003

Abstract
This paper proposes a novel structural health monitoring framework for damage detection of smart structures. The framework is developed through the integration of the discrete wavelet transform, an autoregressive (AR) model, damage-sensitive features, and a support vector machine (SVM). The steps of the method are the following: (1) the wavelet-based AR (WAR) model estimates vibration signals obtained from both the undamaged and damaged smart structures under a variety of random signals; (2) a new damage-sensitive feature is formulated in terms of the AR parameters estimated from the structural velocity responses; and then (3) the SVM is applied to each group of damaged and undamaged data sets in order to optimally separate them into either damaged or healthy groups. To demonstrate the effectiveness of the proposed structural health monitoring framework, a three-story smart building equipped with a magnetorheological (MR) damper under artificial earthquake signals is studied. It is shown from the simulation that the proposed health monitoring scheme is effective in detecting damage of the smart structures in an efficient way.

(Some figures may appear in colour only in the online journal)

1. Introduction

In recent years, smart control technology has been proposed in large-scale structures because the dynamic behavior of a structural system can be modified to counter destructive environmental forces without significantly increasing the mass of the structure (Spencer *et al* 1997, Nagarajaiah and Spencer 2003, Hurlebaus and Gaul 2006, Kim *et al* 2009). However, the performance of the smart control systems can degrade in the presence of sensor/actuator faults and/or structural damage. To address the aforementioned issues, structural health monitoring (SHM) has become increasingly important for large-scale civil infrastructures, because damage affects the current or future performance of the structures (Sharifi *et al* 2010). SHM can provide information when the structures experience any significant change or damage. SHM improves the safety and reliability of critical structures by detecting the damage before they reach a critical state. It also allows rapid damage assessment. In order to practice SHM more efficiently, engineers and researchers have developed various global and local approaches.

In general, SHM can be divided into local and global methods (Chang 2005). The local methodology (also known as the visual method) usually detects damage using local information such as eye inspection, acoustic emission, eddy current scanning, magnetic field methods and the thermal field method, among others. The methods are very sensitive and are able to identify even slight damage. However, it may be challenging to apply the local methods to some applications due to extensive equipment installation and prohibitive costs. In contrast, being a vibration-based method, the global method makes it possible to detect damage using data measured from the structural systems. It can identify structural damage more efficiently when the damage may

be hidden below the surface of the structure. Also, it has the potential to facilitate the more economical management and maintenance of large-scale civil infrastructures. As for the vibration-based SHM, a feature extraction scheme can be used. It identifies damage-sensitive properties, obtained from the structural dynamic responses. One of the effective feature extraction procedures is system identification (SI) using the measured data (Kim *et al* 2009). SI can be used to identify the location and the severity of the damage by constructing mathematical models of dynamic systems from measured data. The SI techniques can be applied to either a set of input and output data or univariate input/output data. In particular, the output-only SI methods, such as an autoregressive model, have become of significance in assessing large-scale civil structures, since the input data (e.g. environmental conditions) are not readily available.

The autoregressive (AR) time series model is one example of using output-based SI methods. Due to its advantage of requiring only the output data from the structure under ambient excitations, time series analysis methods using the AR model are being employed by various researchers (Silva *et al* 2008, Nair *et al* 2006, Ettefagh *et al* 2007, Nair and Kiremidjian 2007, Carden and Brownjohn 2007, Brincker *et al* 1995a, Zheng and Mita 2007, Brincker *et al* 1995b, Kondo and Hamamoto 1996). Once a specific model is established through the time series method, structural damage can be identified. The autoregressive (AR) coefficients of the time series model can represent the dynamics of damage-sensitive features, by observing the changes in the AR coefficients (Nair *et al* 2006, Sohn *et al* 2000, Nair and Kiremidjian 2007, Sohn and Farrar 2000, Lu *et al* 2008, Carden and Brownjohn 2007, Gul and Catbas 2009, Mosavi *et al* 2011). Nair *et al* (2006) have suggested a new damage-sensitive feature which is a function of the first three AR coefficients. They performed a hypothesis test involving the *t*-test to assess the significance of the damage identification. The results provided effective representation of structural damages and their localization within a structural system.

However, all of the aforementioned approaches have been applied based on the assumption that the structure under investigation is linear and time invariant: to date, there is no study on the application of nonlinear and time-varying AR-based SHM schemes to smart structures. In addition, most AR modeling algorithms require intensive computation time to obtain the parameter estimates, which can become a drawback for real time applications. Such a problem can be solved by a discrete multi-resolution wavelet transform. Hence, perhaps it would be informative to cite the work of Daoudi *et al* (1999) on a multi-scale analysis framework. They integrated a multi-scale AR model with all compactly supported wavelets under an assumption that the prediction errors are white. To demonstrate its effectiveness, the multi-scale analysis framework was applied to the problem of estimating a fractional Brownian motion (fBm). However, such a hybrid scheme has not yet been applied to the problem of health monitoring of civil structures equipped with smart control devices.

The wavelet transform (WT) provides a time–frequency representation of the signal through time and scale window functions. The WT reduces computational time, and is also effective in reduction of noise when measured vibration signals are obtained with undesirable noise (Mitchell *et al* 2012a, 2012b). The WT has been used for SHM and damage detection due to its advantages such as data compression and noise reduction (Hou *et al* 2000, Bajaba and Alnefaie 2005, Rucka 2011, Gokdag 2010, Daoudi *et al* 1999). In this paper, the WT is integrated with the AR (WAR) such that the measured data are compressed and de-noised. Hence the AR models can be efficiently constructed. When the WAR model is available from both the undamaged and damaged dynamic systems, a supervised classification approach, the support vector machine (SVM), can be used to detect the damage.

The SVM technique (Vapnik 1995) for solving pattern recognition problems is being considered to classify the target structures as either damaged or healthy. The SVM is based on statistical learning theory, which classifies the given data by finding the optimal hyperplane with the largest margin between the classes in a high dimensional feature space. The SVM has recently been applied for structural damage detection because of its ability to form an accurate boundary and its good generalization capability with large margin scales (Park *et al* 2007, Mita and Hagiwara 2003, Worden and Lane 2001, Shimada and Mita 2005). In this paper, based on the differences in eigenvalues (or poles or AR coefficients) of the damaged and undamaged structures, the damage is identified using the SVM.

This study will be the first attempt to systematically integrate the WT, the AR, the damage-sensitive energy feature (DEF), and the SVM into a single SHM framework for damage detection of smart structures equipped with time-varying nonlinear hysteretic control devices. This paper is organized as follows: first, the wavelet-based autoregressive (WAR) time series model is described in section 2. Section 3 discusses the SVM, followed by simulation results in section 4. Concluding remarks are given in section 5.

2. Wavelet-based AR

In this paper, a novel SHM scheme for damage detection in smart structures is presented as shown in figure 1. First, the discrete wavelet transform (DWT) is applied to the measurements in order to not only reduce the computational time but also reduce noise from the measured data. Then, the AR time series model estimates behavior of structural dynamic systems, based on the wavelet-filtered data. Once the WAR is constructed, the AR coefficients from the WAR model are extracted to identify structural damage. The prediction root mean squared error (RMSE) is minimized by using the least-squares method.

The main advantage of the proposed approach is that it can be applied to structures under ambient vibrations. To apply the proposed method to real structures, two excitation sources will be needed: first, the structures need to be excited by impact hammers, shakers, vehicles or unknown ambient

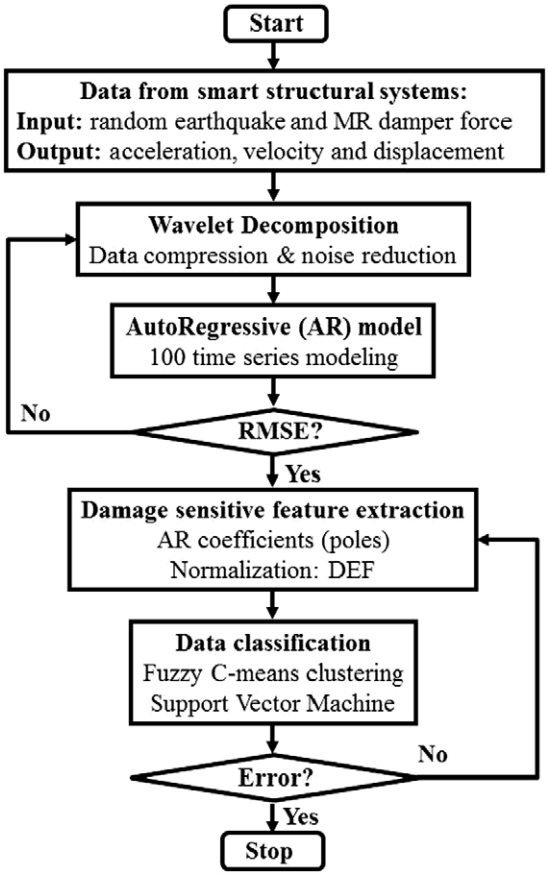

Figure 1. Architecture of the proposed WAR–SVM.

excitation sources. The second excitation is the voltage signal to input to the MR damper, which will be converted into currents using voltage-to-current converters. Based on these excitations, several measurements will be collected, including displacements, velocities, accelerations, and forces. Then, appropriate measurements will be selected to allow the proposed signal processing technique to detect any damage in the structures. However, in real applications, there are many challenging issues. For example, the effects of temperature changes lead to a shift of fundamental frequencies in large civil structures. This may lead to undesirable decision making about structural damage (Sohn *et al* 1998).

2.1. AR model

In general, the AR model is given by

$$\mathbf{y}(n) = \sum_{i=0}^{P} a_i y(n-i) + e(n), \tag{1}$$

where P represents the optimal AR model order. The term $e(n)$ is considered a noise source or prediction-error term. The parameter a_i represents to-be-estimated coefficients of the AR term. The candidate vectors are the following: $y(n-1), \ldots, y(n-P)$. This candidate vector can be arranged as the matrix shown below:

$$\begin{matrix} y(0) & y(-1) & \cdots & y(1-P) \\ y(1) & y(0) & \cdots & y(2-P) \\ \vdots & \vdots & \cdots & \vdots \\ y(n-1) & y(n-2) & \cdots & y(n-P) \\ \vdots & \vdots & \cdots & \vdots \\ y(N-1) & y(N-2) & \cdots & y(N-P), \end{matrix} \tag{2}$$

where N is the total number of data points. With the new candidates for linearly independent vectors, least-squares analysis is performed:

$$\mathbf{y}(n) = \boldsymbol{\theta}_g^{\mathrm{T}} \mathbf{H} + \mathbf{e}(n), \tag{3}$$

where $\mathbf{H} = [h_0, h_1, \ldots, h_R]$, h_i are the selected linearly independent measurements, R is the maximum number of selected vectors and

$$\boldsymbol{\theta}_g = [g_0,\ g_1,\ \ldots,\ g_R]^{\mathrm{T}}, \tag{4}$$

where g_i is the coefficient estimate of the AR model. The objective is to minimize the equation error, $\mathbf{e}(n)$, in the least-squares sense using the criterion function defined as

$$J_N\left(\boldsymbol{\theta}_g\right) = [\mathbf{y}(n) - \boldsymbol{\theta}_g^{\mathrm{T}} \mathbf{H}]^2. \tag{5}$$

The criterion function in (5) is quadratic in $\boldsymbol{\theta}_g$, and can be minimized taking a partial derivative with respect to $\boldsymbol{\theta}_g$, yielding the following well-known least-squares equation:

$$\hat{\boldsymbol{\theta}}_g = [\mathbf{H}\mathbf{H}^{\mathrm{T}}]^{-1} \mathbf{H}\mathbf{y}(n). \tag{6}$$

With the obtained coefficients, we calculate every $|\overline{g_m^2 h_m^2}|$, and rearrange the h_m in descending order. Note that the over-bar represents the time average. At this step of the algorithm, the number of candidate vectors h_m necessary for obtaining proper accuracy needs to be chosen. This approach is taken in order to retain only the h_m that reduce the error value significantly. If either negligible decrease or increase in the error value by adding additional h_m is found, then those h_m are dropped from the model. Once only those h_m that reduce the error value significantly are obtained, the AR model terms are estimated using the least-squares method, as described by Lu *et al* (2001). In order to enhance the efficiency of the AR model, the DWT method is introduced. The integration of the WT method helps not only to reduce the computational time, but also to reduce the amount of data noise.

2.2. Discrete wavelet transform (DWT)

The continuous WT is a time–frequency analysis method which allows arbitrarily high localization of high frequency signal features within the given time. The continuous WT can be defined as

$$W_\psi f(b_{\mathrm{w}}, a_{\mathrm{w}}) = \frac{1}{\sqrt{a_{\mathrm{w}}}} \int_{-\infty}^{\infty} f(t) \psi \left(\frac{t - b_{\mathrm{w}}}{a_{\mathrm{w}}} \right) \mathrm{d}t, \tag{7}$$

where $\psi(t)$ is the wavelet function, and a_{w} and b_{w} represent the scale and the translation parameter, respectively. The

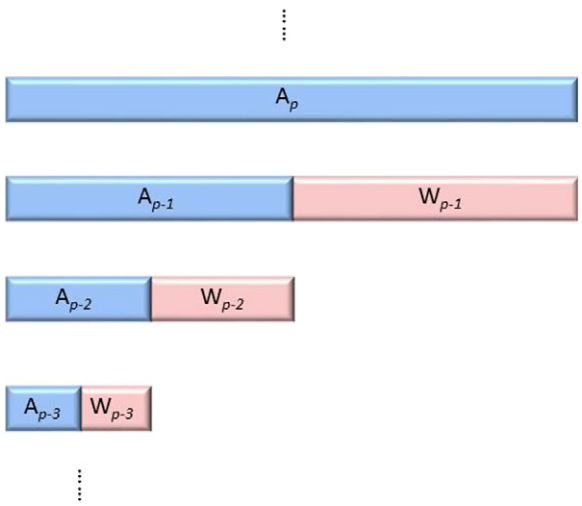

Figure 2. Wavelet transform-based multi-resolution analysis framework.

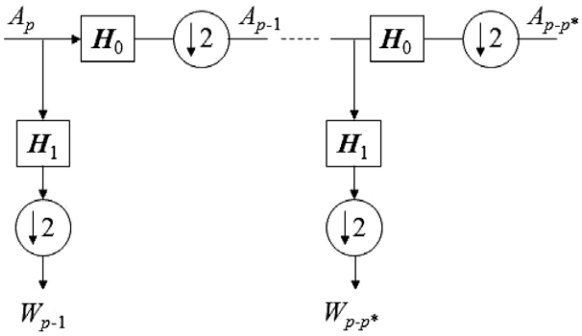

Figure 3. Wavelet transform-based multi-resolution analysis framework.

DWT, which can yield a fast computation of WT, can be derived:

$$W_{s_1,s_2} = 2^{s_1/2} \sum_n f(n)\psi\left(2^{s_1}n - s_2\right), \tag{8}$$

where $f(n)$ is the discrete time signal, and s_1 and s_2 represent the scaling factor and the translation factor, respectively. The WT can be applied to multi-resolution analysis (WMRA) frameworks using wavelet basis functions (Mallat 1989). The WMRA can decompose the structural response signals into sub-components at different resolutions as shown in figure 2.

It decomposes the measured signals into low and high frequency components, which are called approximation (A_p) and detail (W_p) components, respectively. Hence it allows for a representation of the measured responses at a single level of approximation by discretizing the measurement using the step size, and therefore significantly reducing the total number of data points. It is also known as a multi-filter bank (Strang and Nguyen 1996). The multi-filter bank-based wavelet decomposition tree is depicted in figure 3.

In the configuration of the multi-filter bank-based wavelet decomposition, the following vector notation is used:

$$A_p := \{a_{s_1,s_2}\} \tag{9}$$

$$W_p := \{w_{s_1,s_2}\} \tag{10}$$

$$H_0 := \{h_0[s_2]\} \tag{11}$$

$$H_1 := \{h_1[s_2]\} \tag{12}$$

where H_0 and H_1 are convolution operators. The subspaces A_p are generated by $\phi(n) \in L^2(\mathbb{Z})$, called the scaling function, while W_p is generated by the wavelet function $\psi(n) \in L^2(\mathbb{Z})$, where $\mathbb{Z}$ is the set of all integers. The scaling function $\phi(n)$ and the corresponding wavelet $\psi(n)$ are defined by the following dilation equations:

$$\phi_{s_1,s_2} = 2^{s_1/2}\phi(2^{s_1}n - s_2), \tag{13}$$

$$\psi_{s_1,s_2} = 2^{s_1/2}\psi(2^{s_1}n - s_2). \tag{14}$$

The scaling function acts as a low pass filter and also provides an approximation of the original series in the AR modeling process, while the corresponding wavelet acts as a high pass filter and provides the detailed information. The Daubechies scaling function is used. In summary, by removing the detail components ($\boldsymbol{W}_{p-p*}$) from the original signal ($\boldsymbol{A}_p$), some signals that are not related to fundamental characteristics of the dynamic system are filtered, e.g. noise signals. Hence the filtered signal ($\boldsymbol{A}_{p-p*}$) is used for modeling the AR time series models, that is, the wavelet function is not used. This is because we extract the characteristic properties (i.e. the approximation function) of the smart structure, not any damage features (i.e. the detail function) for smart structures. This helps compress the size of the data.

2.3. Wavelet-based AR model

As previously discussed, the WT provides a useful decomposition of the time series in both time and frequency. Thus, when it is incorporated into the AR model, the WT enhances the efficiency of the modeling process. A WAR model is proposed as an integration of the WT into the AR model. The wavelet-based AR can be derived as follows:

$$\hat{y}(n) = \sum_{l_1=0}^{P} a_{l_1} A_{p-p^*}(n - l_1) + e(n). \tag{15}$$

The proposed WAR model uses level two multi-resolution wavelet decomposition. To perform the structural damage detection on smart structures, the AR coefficients are extracted from the AR models.

3. Structural damage detection

3.1. AR coefficients

Any damage to a structure will cause changes in the system stiffness and damping. These changes can be quantitatively measured by observing the AR coefficients. This is because the AR coefficients are correlated with the eigenvalues of dynamic systems. Hence, when the AR coefficients from the damaged and undamaged systems are available, damage-sensitive features can be extracted in order to detect the damage. However, the first few AR coefficients have

limited use for the linear stationary dynamic signals (Nair *et al* 2006). It would not be effective to apply the AR coefficients to the responses measured from the nonlinear time-varying dynamic systems such as structures equipped with nonlinear hysteretic control devices. With this in mind, a new damage-sensitive feature is defined in terms of the AR parameters estimated from the velocity responses of the structure-control system, termed the damage-sensitive energy feature or DEF.

3.2. Damage-sensitive energy feature (DEF)

In this paper, a new damage-sensitive energy feature (DEF) is defined through the grouping of the AR coefficients. Although a number of damage features were considered, dividing the AR parameters into two groups appeared to be the most effective, as it is challenging to extract damage-sensitive features using only the first few AR coefficients obtained from nonlinear dynamic systems. From many trial and error simulations, it was found that the AR coefficients normalized by the pseudo-energy expression provide the most effective damage features. The proposed damage feature is defined as follows:

$$\mathrm{DEF} = \sum_{q}^{P} \tfrac{1}{2} m \left| V_q^E \right|^2, \tag{16}$$

where m is the mass of the structure, V_q^E is the qth AR coefficient, which can be obtained from the velocity responses, and P is the total number of AR coefficients. Note that the velocity is obtained from a Kalman filter estimator, based on three acceleration responses. The effectiveness of the estimator has been demonstrated from previous studies, numerically and experimentally (Dyke *et al* 1998). The value of the mass m is unknown in real applications although it can be roughly estimated using information on dimensions and material densities. Hence, the value of m in real structural applications needs to be determined by trial and error until the healthy and damaged statuses are reasonably visualized. However, m in this application does not need to be an exact representation of the structure's mass. The value of the mass is used only for the normalization process. Note that it would not be easy to identify some damage in the smart structure because many DEF values are collected; in this paper 100 DEF points are obtained from 100 WAR models. To address this issue, an SVM is applied to the sets of DEF values in order to effectively classify the measured data into damaged or undamaged status.

3.3. Support vector machines (SVMs)

SVMs classify data by finding the optimal hyperplane with the largest margin between the classes in a high dimensional feature space (Burges 1998). Consider a training data set S comprising N observations, $\{\mathbf{y}_i\}$, where $i = 1, 2, \ldots, N$ along with corresponding target values $\{T_i\}$ with two separate classes, i.e. $T_i \in \{-1, 1\}$, and the equation of the hyperplane is

$$F_{\mathrm{H}} = \langle \mathbf{w}_s, \phi(\mathbf{y}) \rangle + b_s = 0,$$
$$\mathbf{w}_s \in \mathbb{R}^0, \quad \mathbf{y} \in \mathbb{R}^0, \quad b_s \in \mathbb{R} \tag{17}$$

where $\boldsymbol{y}$ is a zero-dimensional input vector, $\phi(\mathbf{y})$ is a feature-space transformation, $\boldsymbol{w}_s$ is the weight vector, b_s is the bias, and $\langle \boldsymbol{w}_s, \phi(\boldsymbol{y}) \rangle$ is the inner product of $\boldsymbol{w}_s$ and $\boldsymbol{y}$. The optimal separating hyperplane is the hyperplane that separates S by concentrating all points within the same class on one side while maximizing the margin, which is the distance between the closest points of the divided classes. This closest vector $\boldsymbol{y}_i$ is called the support vector. SVMs can be categorized into linear and nonlinear.

Linear SVMs can be classified into hard-margin SVMs and soft-margin SVMs (Mainmon and Rokach 1980). A hard-margin SVM ensures that the maximum margin classifier classifies correctly, under the condition that the data are separable. The equation for finding the support vectors and their optimized separating hyperplane for hard-margin SVM is defined as follows.

$$\begin{aligned} &\text{Minimize} \quad d(\mathbf{w}_s) = \tfrac{1}{2}\langle \mathbf{w}_s, \mathbf{w}_s \rangle. \\ &\text{Subject to} \quad T_i(\langle \mathbf{w}_s, \mathbf{y}_i \rangle + b_s) \geq 1, \quad \text{for } i = 1, 2, \ldots, N. \end{aligned} \tag{18}$$

Since data are often not linearly separable, soft-margin SVMs introduce the idea of slack variables $\delta_i = |T_i - F_{\mathrm{H}}(\mathbf{y_i})|$ and the tradeoff between maximizing the margin and minimizing the number of misclassified variables by the parameter C_s. The equation for finding the support vector and its optimized separating hyperplane for the soft-margin SVM is defined as follows.

$$\begin{aligned} &\text{Minimize} \quad d(\mathbf{w}_s) = \tfrac{1}{2}\langle \mathbf{w}_s, \mathbf{w}_s \rangle + C_s \sum \delta_i \\ &\text{Subject to } T_i(\langle \mathbf{w}_s, \mathbf{y}_i \rangle + b_s) \geq 1 - \delta_i, \\ &\qquad \text{for } i = 1, 2, \ldots, N, \ \text{for } \delta_i \geq 0. \end{aligned} \tag{19}$$

The application of a linear SVM can be further extended to build a nonlinear SVM. The concept of nonlinear SVM is to allow an SVM with a nonlinear decision surface to classify nonlinearly separable data. For a nonlinear SVM, each input data point $\boldsymbol{y}_i$ is transformed into a feature space using a nonlinear mapping $\boldsymbol{y}_i \rightarrow \Phi(\boldsymbol{y}_i)$. The classification constraints in (19) are replaced with

$$T_i(\langle \mathbf{w}_s, \Phi(\mathbf{y}_i) \rangle + b_s) \geq 1, \qquad \text{for } i = 1, 2, \ldots, N. \tag{20}$$

A kernel function K_s is a function that corresponds to a dot product in some expanded feature space. The benefit of the kernel function is that, as the original input vectors appear only in terms of inner products, the kernel function can be calculated without knowing $\Phi(\mathbf{y}_i)$ explicitly:

$$K_s(\mathbf{y_i}, \mathbf{y_j}) = \langle \Phi(\mathbf{y}_i), \Phi(\mathbf{y}_j) \rangle. \tag{21}$$

Among the possible function candidates, the Gaussian radial basis function is used to assess the damage of a structure:

$$K_s(\mathbf{y_i}, \mathbf{y_j}) = \exp\left(-\frac{\|\mathbf{y}_i - \mathbf{y}_j\|^2}{2\sigma^2} \right). \tag{22}$$

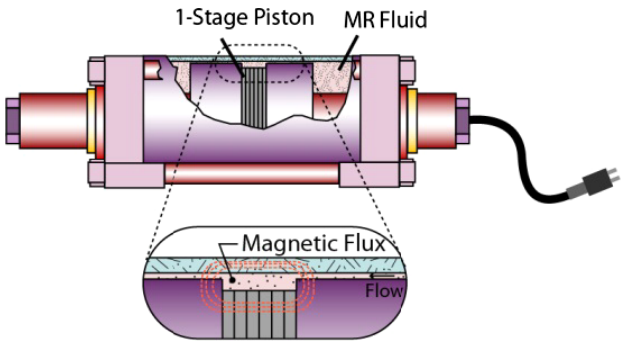

Figure 4. MR damper.

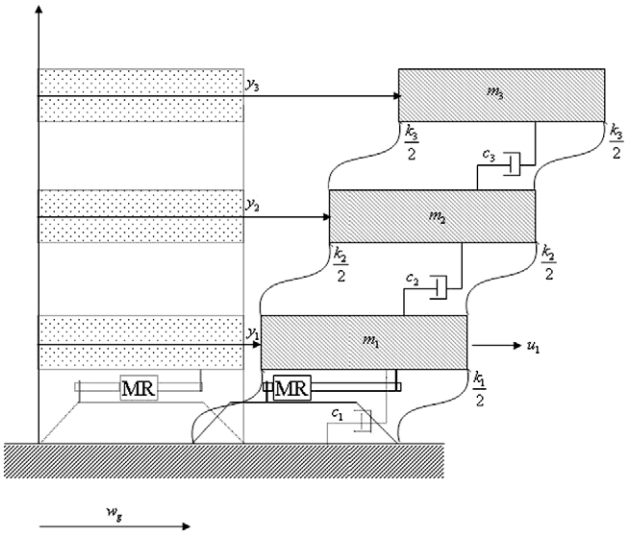

Figure 5. Smart building equipped with MR dampers.

In order to demonstrate the effectiveness of the nonlinear wavelet-based AR–SVM classification technique, a three-story building equipped with an MR damper is investigated.

4. Case study

4.1. A structure equipped with magnetorheological (MR) dampers

To demonstrate the effectiveness of the proposed WAR–SVM framework, a three-story building structure employing MR dampers was investigated (Kim *et al* 2009). It was a laboratory model (Dyke *et al* 1996) of a prototype building structure that was developed by Chung *et al* (1989). The MR damper is one of the promising semi-active control devices for structural vibration reduction that combines the best features of both active and passive control systems. An MR damper is filled with MR fluids and controlled by a magnetic field as shown in figure 4.

When a magnetic field is applied to the MR fluids, the MR fluids are changed into a semi-solid state in a few milliseconds. A typical example of a building structure employing an MR damper is shown in figure 5.

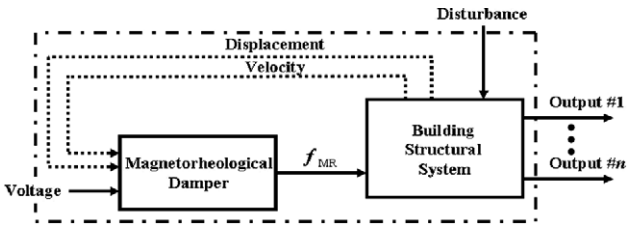

Figure 6. Integrated building structure–MR damper system.

The equation of motion of the structure is defined as

$$\mathbf{M}\ddot{\mathbf{y}}_s + \mathbf{C}\dot{\mathbf{y}}_s + \mathbf{K}\mathbf{y}_s = \Gamma\mathbf{f}_{\mathbf{MR}}(t, y_{s1}, \dot{y}_{s1}, v_1) - \mathbf{M}\Lambda\ddot{w}_g, \quad (23)$$

where $\ddot{w}_g$ represents the ground acceleration, $\mathbf{M}$ the mass matrix, $\mathbf{K}$ the stiffness matrix, and $\mathbf{C}$ the damping matrix. The vector $\mathbf{y}_s$ is the displacement relative to the ground, $\dot{\mathbf{y}}_s$ the velocity, $\ddot{\mathbf{y}}_s$ the acceleration; $\mathbf{y}_i$ and $\dot{\mathbf{y}}_i$ are the displacement and the velocity at the ith floor level relative to the ground, respectively, v_i is the voltage level to be applied, and Γ and $\mathbf{\Lambda}$ are the location vectors of control forces and the disturbance signal, respectively. Figure 6 shows the configuration of the integrated building–MR damper system.

The second order differential equation can be converted into a state space model:

$$\begin{aligned}\dot{\mathbf{z}}_s &= \mathbf{A}^*\mathbf{z}_s + \mathbf{B}^*\mathbf{f}_{\mathbf{MR}}(t, z_{s1}, z_{s4}, v_1) - \mathbf{E}^*\ddot{w}_g \\ \mathbf{y} &= \mathbf{C}^*\mathbf{z}_s + \mathbf{D}^*\mathbf{f}_{\mathbf{MR}}(t, z_{s1}, z_{s4}, v_1) + \mathbf{n},\end{aligned} \quad (24)$$

where

$$\mathbf{A}^* = \begin{bmatrix} \mathbf{0} & \mathbf{I} \\ -\mathbf{M}^{-1}\mathbf{K} & -\mathbf{M}^{-1}\mathbf{C} \end{bmatrix}, \quad (25)$$

$$\mathbf{B}^* = \begin{bmatrix} \mathbf{0} \\ \mathbf{M}^{-1}\mathbf{F} \end{bmatrix}, \quad (26)$$

$$\mathbf{C}^* = \begin{bmatrix} \mathbf{I} & \mathbf{0} \\ \mathbf{0} & \mathbf{I} \\ -\mathbf{M}^{-1}\mathbf{K} & -\mathbf{M}^{-1}\mathbf{C} \end{bmatrix}, \quad (27)$$

$$\mathbf{D}^* = \begin{bmatrix} \mathbf{0} \\ \mathbf{0} \\ \mathbf{M}^{-1}\mathbf{F} \end{bmatrix}, \quad (28)$$

$$\mathbf{E}^* = \begin{bmatrix} \mathbf{0} \\ \mathbf{F} \end{bmatrix}, \quad (29)$$

$\mathbf{F}$ is the location matrix of where chevron braces are located within the building structure, and $\mathbf{n}$ is the noise vector. The properties of a three-story building structure are given: the mass of each floor $m_1 = m_2 = m_3 = 98.3$ kg; the stiffness of each story $k_1 = 516\,000$ N m^{-1}, $k_2 = 684\,000$ N m^{-1} and $k_3 = 684\,000$ N m^{-1}; and damping coefficients of each floor $c_1 = 125$ N s m^{-1}, $c_2 = 50$ N s m^{-1} and $c_3 = 50$ N s m^{-1}. The properties of the SD-1000 MR damper are given by table 1. Based on this building–MR damper system, a set of dynamic responses is collected for use in modeling the WAR model.

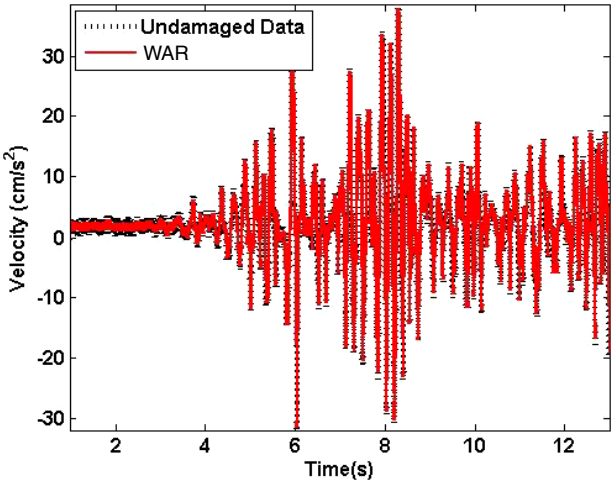

Figure 7. Comparison of the WAR model and healthy data from smart structures.

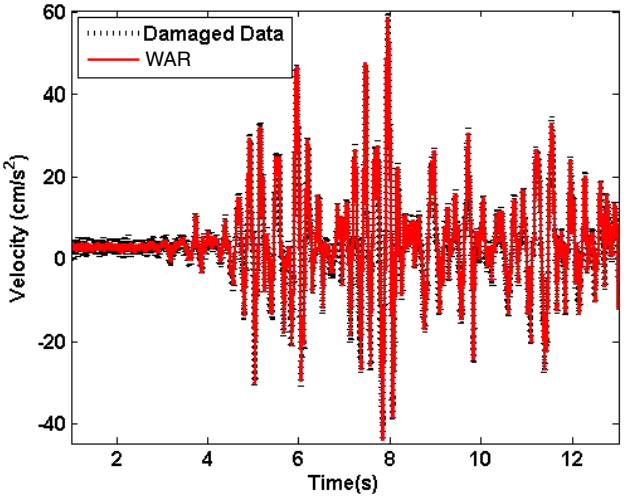

Figure 8. Comparison of the WAR model and damaged data from smart structures.

Table 1. Parameters for SD-1000 MR damper model.

Parameter	Value	Parameter	Value
c_{0a}	21.0 N s cm^{-1}	α_a	140 N cm^{-1}
c_{0b}	3.50 N s cm^{-1} V^{-1}	α_b	695 N cm^{-1} V^{-1}
k_0	46.9 N cm^{-1}	γ	363 cm^{-2}
c_{1a}	283 N s cm^{-1}	β	363 cm^{-2}
c_{1b}	2.95 N s cm^{-1} V^{-1}	A	301
k_1	5.00 N cm^{-1}	N	2
x_0	14.3 cm	η	190 s^{-1}

4.2. System identification using the WAR models

To construct the WAR models, a random artificial earthquake and a pseudo-random binary signal are applied to the structure–MR damper system as input disturbance and control current signals, respectively. Figure 7 represents one of 100 WAR models of the undamaged smart structure, while figure 8 represents one of 100 WAR models of the damaged smart structure.

As shown in these figures, good agreement between the proposed WAR model and the original data is found. In addition, to quantify the performance evaluation, RMSE and the fitting rate (FR) are used. As the first evaluation index, the RMSE is given by

$$J_1 = \text{RMSE} = \sqrt{\frac{\sum |\hat{y} - \tilde{y}|^2}{N}}, \tag{30}$$

where $\hat{y}$ is the estimation, $\tilde{y}$ is the actual structural response data, and N is the number of data points. As the second evaluation index, the fitting rate (FR) is used:

$$J_2 = \text{FR} = \left[1 - \frac{\text{var}\,(\tilde{y} - \hat{y})}{\text{var}\,(\tilde{y})}\right] \times 100. \tag{31}$$

If the trained model produces the same responses as the original data, the FR is 100. Table 2 provides the training results, including the error of the trained model and the actual response of the smart structure using the AR model and WAR model.

Table 2. Training results and error.

		Average training time (s)	J_1	J_2
AR	Undamaged system	6.1673	0.0301	93.1530
	Damaged system	6.2890	0.0380	93.3555
WAR	Undamaged system	1.4173	0.0584	95.8929
	Damaged system	1.4085	0.0549	96.1184

Table 3. C^* obtained by fivefold cross-validation and grid search method.

Scenario	Value
50% stiffness at 1st floor	128
30% stiffness at 1st floor	128
15% and 10% stiffness at 1st floor	10
5% stiffness at 1st floor	128
50%, 30%, 10%, 15% and 5% stiffness at 2nd floor	10

Table 4. (C^*, σ^*) obtained by fivefold cross-validation and grid search method.

Scenario	Value
50% stiffness at 1st floor	(10, 0.25)
30%, 15% and 10% stiffness at 1st floor	(10, $\sqrt{2}$)
5% stiffness at 1st floor	(10, 0.5)
50%, 30%, 10%, 15% and 5% stiffness at 2nd floor	(10, $\sqrt{2}$)

The WAR model holds its advantage against the AR model in terms of computational loads and the modeling accuracy, i.e. the computation of the WAR only requires about 20% of the AR model's training time with the better fitting rate; the fitting rate of the WAR model is more than 95% while that of the AR is about 93%. It should be noted that, even with the computational load reduction, the WAR model has a very

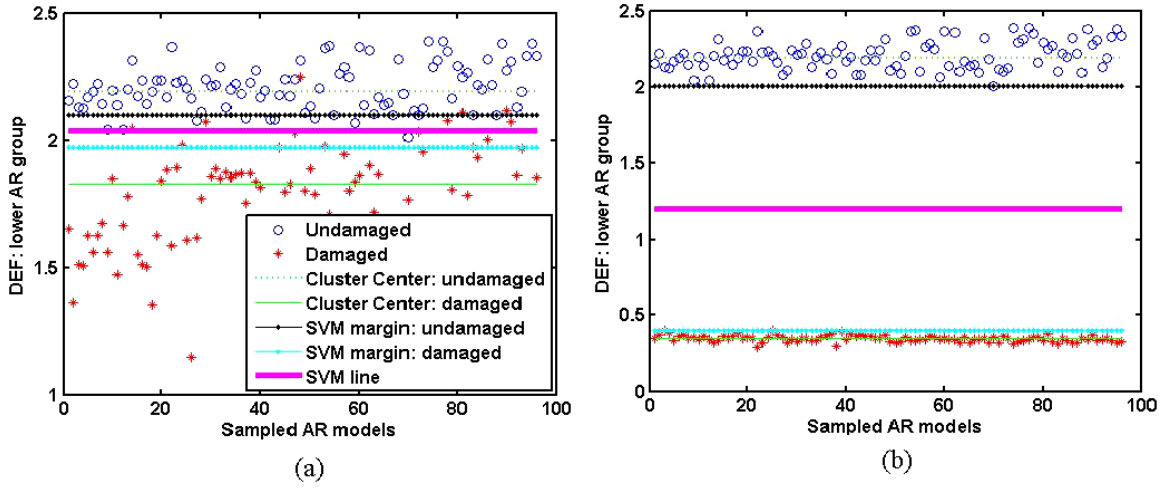

Figure 9. Class cluster centers, margins and decision making lines of the DEF distributions for 50% stiffness degradation. (a) 50% degradation of the first floor stiffness and (b) 50% degradation of the second floor stiffness.

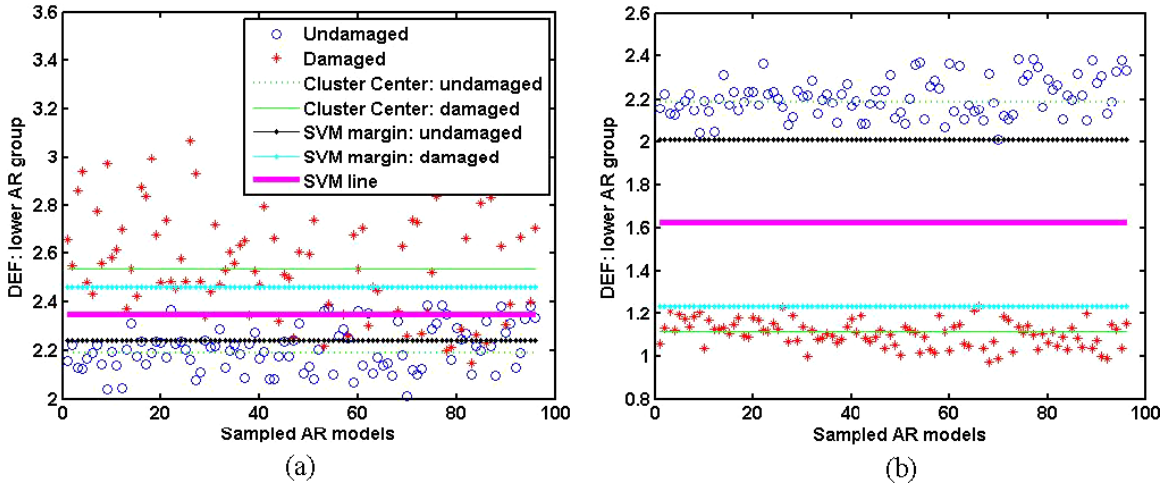

Figure 10. Class cluster centers, margins and decision making lines of the DEF distributions for 30% stiffness degradation. (a) 30% degradation of the first floor stiffness and (b) 30% degradation of the second floor stiffness.

high fitting rate. Thus, the WAR model is used in detecting structural damage in smart structures.

4.3. Structural damage detection

Based on the estimated WAR time series models, the DEFs are extracted through the comparison between damaged and undamaged states of the smart structure using our proposed equation (15). The cluster center values of each group are calculated using the fuzzy C-means clustering algorithm (Kim *et al* 2011). The decision making depends on whether or not the system is damaged and the associated margins are derived using the SVM. In order for the SVM to separate the training datasets into classes with the least possible error, the best SVM kernel and its parameters must be selected. In order to select the best SVM kernel and its parameters, the performance evaluation of each kernel on various parameters requires many trials and errors. If the target class that is predicted differs from the known label of the point, that target class can be classified as an error. By obtaining the errors for a given number of test points, the error rate is evaluated. The error rate is an indication of the SVM's ability to predict the damage in a structure. Therefore, the effect of the kernel parameter (σ) and regularization parameter (C) on the SVM boundary with the lowest error rate is considered, and the parameters with the lowest error accuracy rate using cross-validation and grid search are chosen (Hsu *et al* 2010). For one-dimensional DEF classification (i.e. related to the first 10 AR coefficients) a linear kernel with $C = 2^{-5}, \ldots, 2^{15}$ is considered in fivefold cross-validation to obtain the SVM boundary, while for two-dimensional DEF classification (i.e. related to both the first 10 AR and the first 100 AR parameters) a Gaussian kernel with various grid pairs of (C, σ), where $C = 2^{-5}, \ldots, 2^{15}$ and $\sigma = 2^{-15}, \ldots, 2^{15}$, is considered. The obtained parameters for one- and two-dimensional DEF classifications are listed in tables 3 and 4, respectively. After acquiring the most suitable kernel and its parameters, the dataset can then be classified by the SVM.

Figures 9–13 show the results from the application of the proposed DEF and the SVM algorithms to the smart structures with stiffness degradations of 50%, 30%, 15% and 5%. In

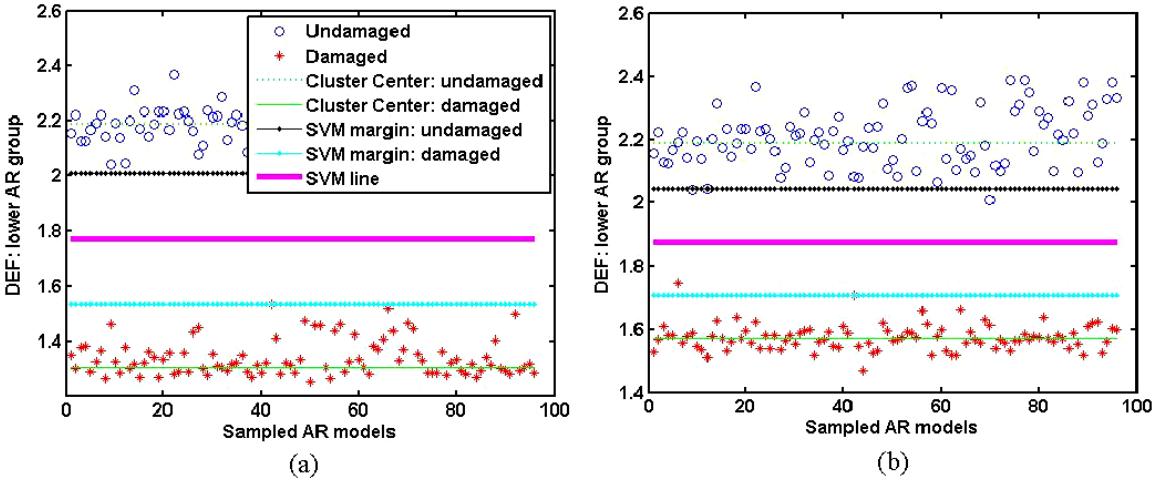

Figure 11. Class cluster centers, margins and decision making lines of the DEF distributions for 15% stiffness degradation. (a) 15% degradation of the first floor stiffness and (b) 15% degradation of the second floor stiffness.

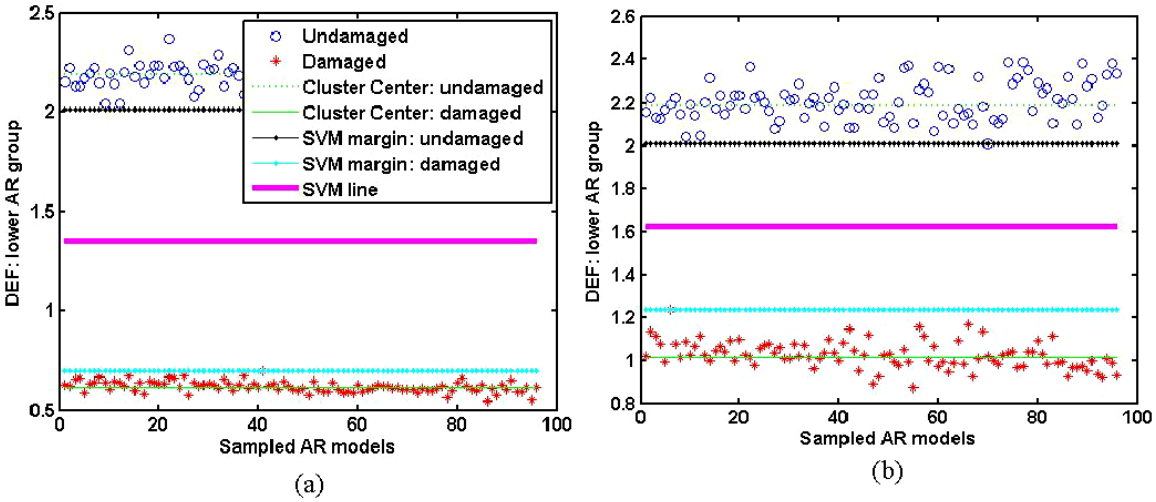

Figure 12. Class cluster centers, margins and decision making lines of the DEF distributions for 10% stiffness degradation. (a) 10% degradation of the first floor stiffness and (b) 10% degradation of the second floor stiffness.

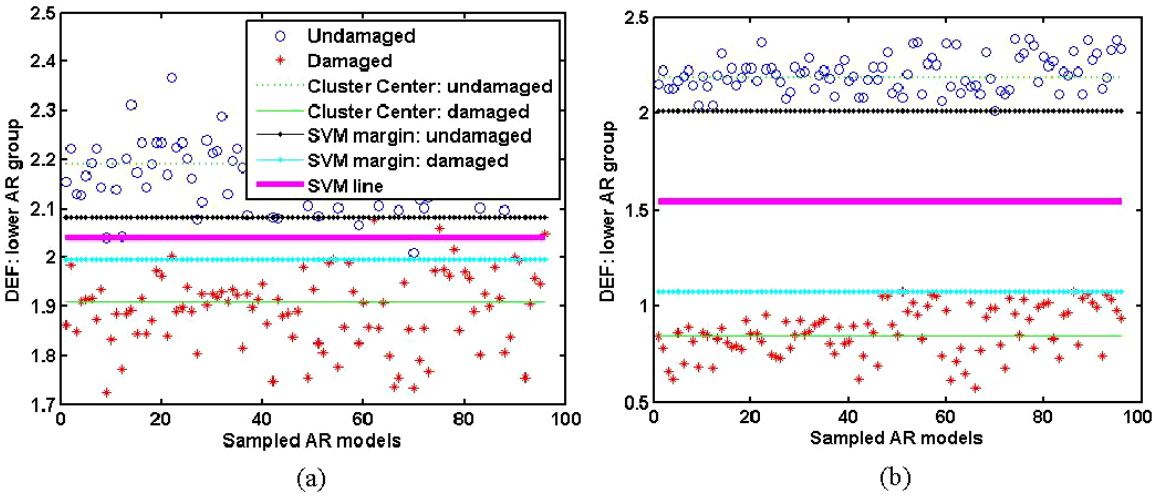

Figure 13. Class cluster centers, margins and decision making lines of the DEF distributions for 5% stiffness degradation. (a) 5% degradation of the first floor stiffness and (b) 5% degradation of the second floor stiffness.

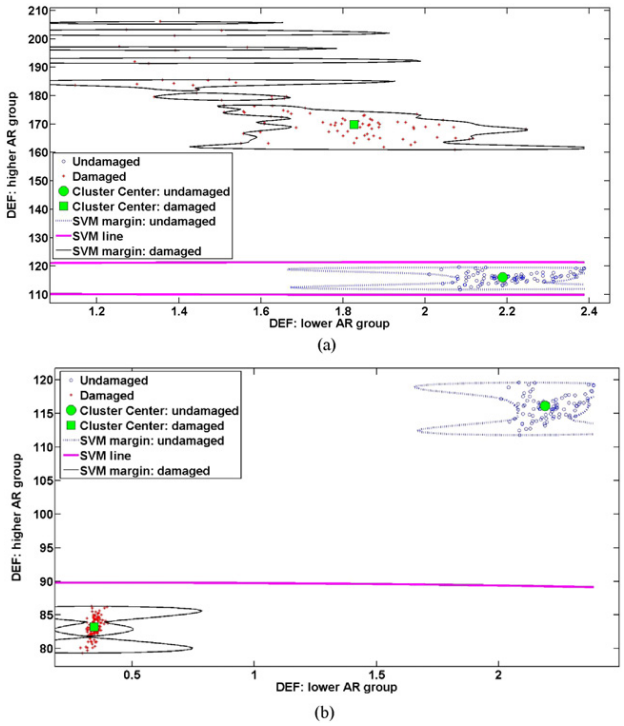

Figure 14. Relationship between the lower and higher AR groups. (a) 50% stiffness degradation at the first floor and (b) 50% stiffness degradation at the second floor.

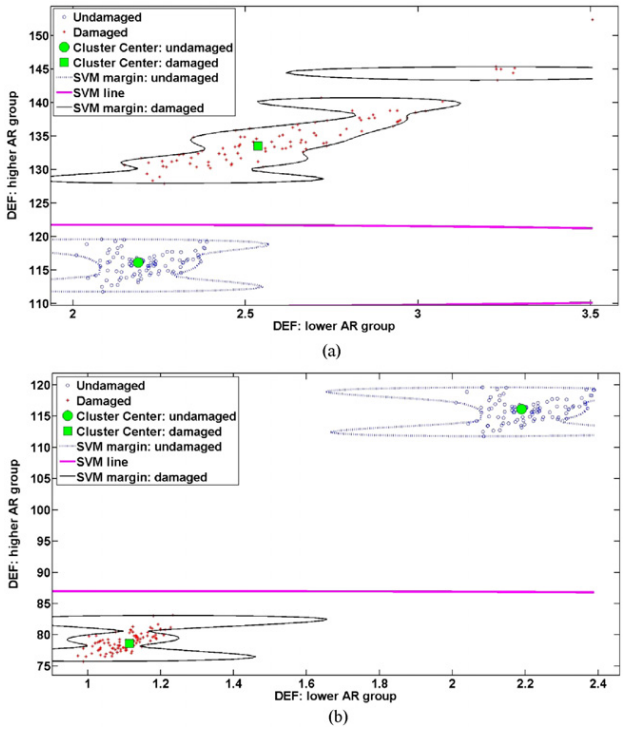

Figure 15. Relationship between the lower and higher AR groups. (a) 30% stiffness degradation at the first floor and (b) 30% stiffness degradation at the second floor.

each figure, (a) and (b) represent the first and second floor damage cases, respectively.

As shown in the figures, the proposed DEF effectively identifies the damage cases, except the 50% and 30% damage

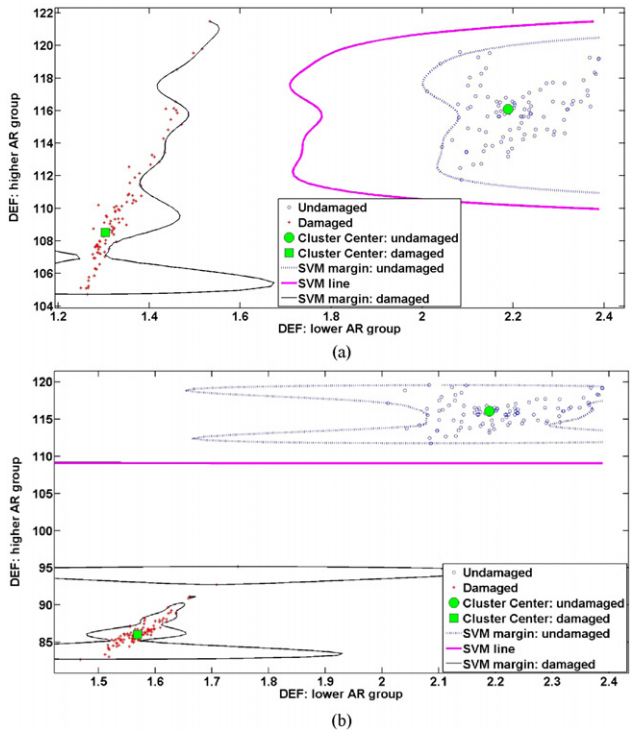

Figure 16. Relationship between the lower and higher AR groups. (a) 15% stiffness degradation at the first floor and (b) 15% stiffness degradation at the second floor.

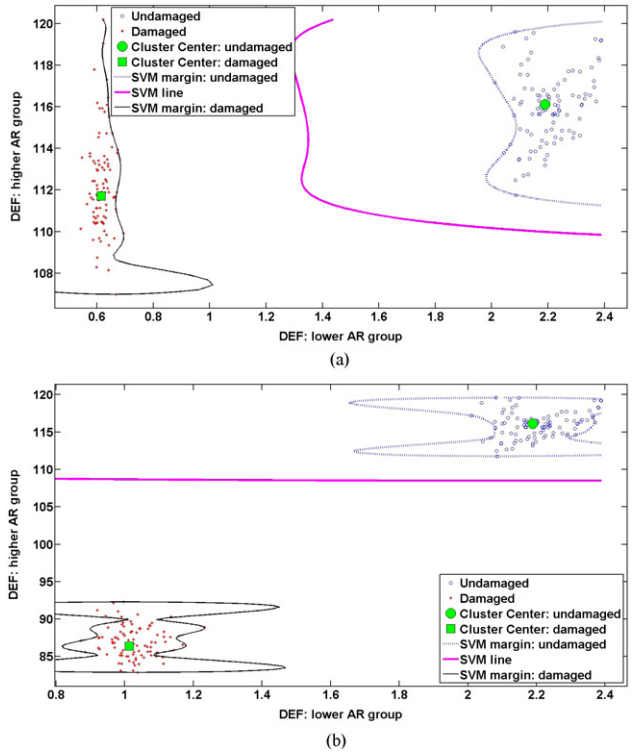

Figure 17. Relationship between the lower and higher AR groups. (a) 10% stiffness degradation at the first floor and (b) 10% stiffness degradation at the second floor.

cases at the first floor level. However, such issues can be addressed by visualizing the relationship between the first AR group (i.e. the summation of the first to tenth AR parameters)

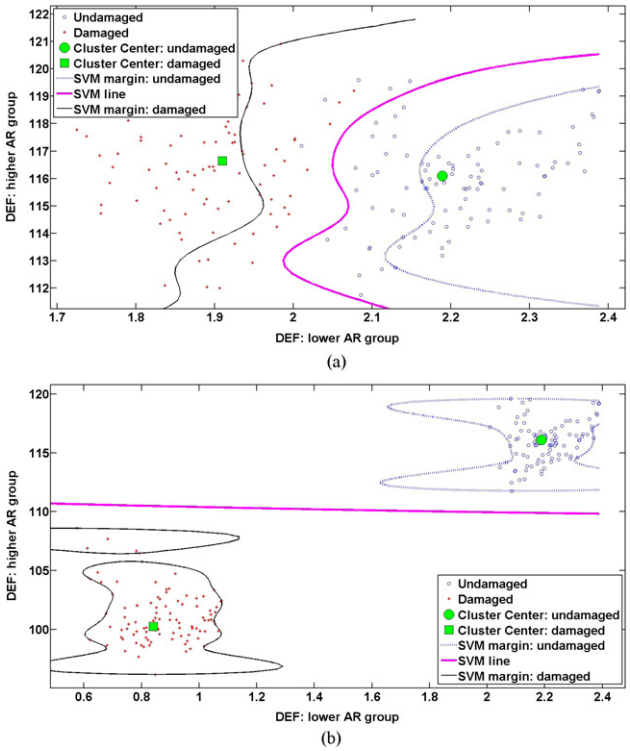

Figure 18. Relationship between the lower and higher AR groups. (a) 5% stiffness degradation at the first floor and (b) 5% stiffness degradation at the second floor.

and the second AR group (i.e. the summation of the first to 100th AR parameters). Figures 14–18 show such relationships between each group of the AR parameters. As shown in the figures, all the structural damage features can be identified. It is shown in these figures that the damage in smart structures can be more clearly discerned by finding the cluster centers and margins.

5. Conclusion

This paper proposes a novel structural health monitoring (SHM) scheme for damage detection of smart structures undergoing destructive environmental forces by employing time-varying nonlinear hysteretic control devices. The SHM framework is developed through the integration of discrete wavelet transform (DWT), autoregressive moving average models (AR), and a new damage-sensitive feature and support vector machine (SVM). The method is as follows: (1) based on ambient excitation-based nonlinear dynamic responses, wavelet-based AR (WAR) time series models are constructed. (2) From the WAR models derived from both the damaged and undamaged structural systems, damage-sensitive energy features (DEFs) are extracted in terms of the AR coefficients, which are related to the eigenvalues of smart structures. (3) The damage is detected by observing the migration of the extracted AR coefficients and SVM. To demonstrate the effectiveness of the proposed WAR–SVM health monitoring framework, a three-story building equipped with a magnetorheological (MR) damper was studied. It is demonstrated from the simulation that the proposed SHM framework is effective in identifying the damage of smart structural systems equipped with time-varying nonlinear MR dampers.

Acknowledgment

This work was partially supported by the National Research Foundation of Korea Grant funded by the Korean Government (NRF-2009-352-D00197).

References

Aggarwal R, Singh J K, Gupta V K, Rathore S, Tiwari M and Khare A 2011 Noise reduction of speech signal using wavelet transform with modified universal threshold *Int. J. Comput. Appl.* **20** 14–9

Bajaba N S and Alnefaie K A 2005 Multiple damage detection in structures using wavelet transforms *Emirates J. Eng. Res.* **10** 35–40

Brincker R, Andersen P, Kirkegaard P H and Ulfkjaer J P 1995a Damage detection in laboratory concrete beams *Proc. 13th Int. Modal Analysis Conf. (Nashville, Tennessee)*

Brincker R, Kirkegaard P H and Andersen P 1995b Damage detection in an offshore structure *Proc. 13th Int. Modal Analysis Conf. (Nashville)*

Burges C J C 1998 A tutorial on support vector machines for pattern recognition *Data Min. Know. Discov.* **2** 121–67

Carden P E and Brownjohn J M W 2007 ARMA modelled time series classification for structural health monitoring *Mech. Syst. Signal Process.* **22** 295–314

Chang F K 2005 *Structural Health Monitoring* (Lancaster: DEStech publications)

Chung L L, Lin R C, Soong T T and Reinhorn A M 1989 Experiments on active control for MDOF seismic structures *ASCE J. Eng. Mech.* **115** 1609–27

Daoudi K, Frakt A B and Willsky A S 1999 Multiscale autoregressive models and wavelets *IEEE Trans. Inf. Theory* **45** 828–45

Dyke S J, Spencer B F Jr, Sain M K and Carlson J D 1996 Modeling and control of magnetorheological dampers for seismic response reduction *Smart Mater. Struct.* **5** 565–75

Dyke S J, Spencer B F Jr, Sain M K and Carlson J D 1998 An experimental study of MR dampers for seismic protection *Smart Mater. Struct.* **7** 693–703

Ettefagh M M, Sadeghi M H and Khanmohammadi S 2007 Structural damage detection using fuzzy classification and ARMA parametric modeling *Mech. Aerosp. Eng. J.* **3** 85–98

Gokdag H 2010 Wavelet-based damage detection method for beam-like structures *Gazi Univ. J. Sci.* **23** 339–49

Gul M and Catbas F N 2009 A modified time series analysis for identification, localization, and quantification of damage *Proc. IMAC-XXVII (Orlando, FA)*

Hou Z, Noori M and Arnand R S 2000 Wavelet-based approach for structural damage detection *J. Eng. Mech.* **126** 665–777

Hsu C-W, Chang C-C and Lin C-J 2010 A practical guide to support vector classification *Technical Report* Department of Computer Science, National Taiwan University

Hurlebaus S and Gaul L 2006 Smart structure dynamics *Mech. Syst. Signal Process.* **20** 255–81

Kim Y, Hurlebaus S, Sharifi R and Langari R 2009 Nonlinear identification of MIMO smart structures *ASME Dynamic Systems and Control Conf. (Hollywood, CA, Oct. 12–14 2009)*

Kim Y, Kim C and Langari R 2010 Novel bio-inspired smart control for hazard mitigation of civil structures *Smart Mater. Struct.* **19** 115009

Kim Y, Langari R and Hurlebaus S 2009 Semiactive nonlinear control of a building structure equipped with a magnetorheological damper system *Mech. Syst. Signal Process.* **23** 300–15

Kim Y, Langari R and Hurlebaus S 2011 MIMO fuzzy identification of building–MR damper systems *Int. J. Intell. Fuzzy Syst.* **22** 185–205

Kondo I and Hamamoto T 1996 Seismic damage detection of multi-story buildings using vibration monitoring *11th World Conf. on Earthquake Engineering (San Francisco)*

Lakshmikantham V and Trigiante D 2002 *Theory of Difference Equations: Numerical Methods and Applications* (New York: Dekker)

Lu K C, Loh C H, Yang Y S, Lynch J P and Law K H 2008 Real-time structural damage detection using wireless sensing and monitoring system *Smart Struct. Syst.* **4** 759–78

Lu S, Ju K H and Chon K H 2001 A new algorithm for linear and nonlinear ARMA model parameter estimation using affine geometry *IEEE Trans. Biomed. Eng.* **48** 1116–24

Mainmon O and Rokach L 1980 *Handbook, Data Mining and Knowledge Discovery* (New York: Springer)

Mallat S G 1989 A theory for multiresolution signal decomposition: the wavelet representation *IEEE Trans. Pattern Anal. Mach. Intell.* **11** 674–93

Mita A and Hagiwara H 2003 Quantitative damage diagnosis of shear structures using support vector machine *KSCE J. Civ. Eng.* **7** 683–9

Mitchell R, Kim Y, El-Korchi T and Cha Y 2012a Wavelet-neuro-fuzzy control of hybrid building-active tuned mass damper system under seismic excitations *J. Vib. Control* at press

Mitchell R, Kim Y and El-Korchi T 2012b System identification of smart buildings using WANFIS model framework *J. Smart Mater. Struct.* **21** 115009

Mosavi A A, Dickey D, Seracino R and Rizkalla S 2011 Identifying damage locations under ambient vibrations utilizing vector autoregressive models and Mahalanobis distances *Mech. Syst. Signal Process.* at press

Nair K K and Kiremidjian A S 2007 Time series based structural damage detection algorithm using Gaussian mixtures modeling *J. Dyn. Syst. Meas. Control* **129** 285–93

Nair K K, Kiremidjian A S and Law K H 2006 Time series-based damage detection and localization algorithm with application to the ASCE benchmark structure *J. Sound Vib.* **291** 349–68

Nagarajaiah S and Spencer B F Jr 2003 State of the art of structural control *ASCE J. Struct. Eng.* **129** 845–56

Park S, Lee J J, Yun C B and Inman D J 2007 A built-in active sensing system-based structural health monitoring technique using statistical pattern recognition *J. Mech. Sci. Technol.* **21** 896–902

Rucka M 2011 Damage detection in beams using wavelet transform on higher vibration modes *J. Theor. Appl. Mech.* **49** 339–417

Sharifi R, Kim Y and Langari R 2010 Sensor fault isolation and detection of smart structures *Smart Mater. Struct.* **19** 105001

Shimada M and Mita A 2005 Damage assessment of bending structures using support vector machine *Proc. SPIE* **5765** 923–30

Silva S D, Junior M D, Junior V L and Brennan M J 2008 Structural damage detection by fuzzy clustering *Mech. Syst. Signal Process.* **22** 1636–49

Sohn H, Czarnecki J A and Farrar C R 2000 Structural health monitoring using statistical process control *ASCE J. Struct. Eng.* **126** 1356–63

Sohn H, Dzwonczyk M, Straser E G, Law K H, Meng T and Kiremidjian A S 1998 Adaptive modeling of environmental effects in modal parameters for damage detection in civil structures *Smart Systems for Bridges, Structures, and Highways; Proc. SPIE* **3** 127–38

Sohn H and Farrar C R 2000 Statistical process control and projection techniques for structural health monitoring *European COST F3 Conf. on System Identification and Structural Health Monitoring (Madrid)*

Spencer B F Jr, Dyke S J, Sain M K and Carlson J D 1997 Phenomenological model for magnetorheological dampers *ASCE J. Eng. Mech.* **123** 230–8

Strang G and Nguyen T 1996 *Wavelet and Filter Banks* (Wellesley, MA: Wellesley-Cambridge Press)

Taha M M R 2010 A neural-wavelet technique for damage identification in the ASCE benchmark structure using phase II experimental data *Adv. Civ. Eng.* **2010** 1–13

Vapnik V 1995 *The Nature of Statistical Learning Theory* (New York: Springer)

Worden K and Lane A J 2001 Damage identification using support vector machines *Smart Mater. Struct.* **10** 540–7

Wu C J, Fu T H and Wu C W 2002 Discrete wavelet transform applied to data compression of waveforms with harmonics and voltage flicker *IEEE Power Eng. Soc. Winter Mtg* **2** 1141–6

Zheng H and Mita A 2007 Damage indicator defined as the distance between ARMA models for structural health monitoring *Struct. Control Health Monit.* **15** 992–1005